

Biexcitons in the semiconductor Cu₂O: An explanation of the rapid decay of excitons

J. I. Jang and J. P. Wolfe

Physics Department and Frederick Seitz Materials Research Laboratory, University of Illinois at Urbana-Champaign,
1110 West Green Street, Urbana, Illinois 61801, USA

(Received 15 March 2005; published 13 December 2005)

Excitons in the semiconductor Cu₂O exhibit a puzzling density-dependent lifetime that severely limits the attainable gas density. Our previous experimental work on this nearly ideal gas points to an anomalously strong Auger recombination process. The observed exciton decay rate is over five orders of magnitude larger than present theoretical estimates indicate for this crystal. Based on time- and space-resolved photoluminescence studies, we propose that the exciton densities are limited by their binding into short-lived excitonic molecules.

DOI: 10.1103/PhysRevB.72.241201

PACS number(s): 71.35.Cc, 71.35.Gg, 73.20.Mf

The search for Bose-Einstein condensation (BEC) of excitons in bulk semiconductors has met with a variety of barriers. In indirect-gap semiconductors such as Si and Ge, these bound electron-hole pairs condense into electron hole liquid before BEC densities can be achieved. Direct-gap semiconductors, on the other hand, have short radiative lifetimes that usually preclude the cooling of the excitonic gas to sufficiently low temperatures. The semiconductor Cu₂O seemingly avoids these maladies due to its forbidden direct gap and a large exciton binding energy, 153 meV. Indeed, at high excitation levels photoluminescence spectra of excitons in high purity Cu₂O crystals display kinetic-energy distributions that closely resemble Bose-Einstein statistics.¹⁻³ Calibration of the luminescence intensities and gas volume, however, showed that the gas density remains less than about 1% of that required for BEC, implying classical statistics.⁴⁻⁶

The quantumlike distributions of excitons in Cu₂O has been explained by spatial inhomogeneities in gas density and temperature, facilitated by a strong Auger recombination of the excitons.⁶ In this two-body process, one exciton recombines while ionizing the other, heating up the gas.⁷⁻⁹ In simple terms, let n be the density of excitons, τ their lifetime against recombination at an impurity, and A the Auger constant. Following a short excitation pulse, the gas density obeys the following rate equation:

$$\frac{dn}{dt} = -\frac{n}{\tau} - An^2. \quad (1)$$

At high initial density the gas exhibits a fast decay rate, An , followed by a slower loss rate τ^{-1} , qualitatively similar to the luminescence decay curve shown in Fig. 1(a). Absolute determination of A requires a measurement of the exciton gas volume $V(t)$ and an optical calibration of the absolute exciton number, $N(t)$. The gas volume is determined from time-resolved imaging of the diffusing exciton cloud,⁵ as illustrated in Fig. 2. The instantaneous gas density is $n(t) = N(t)/V(t)$.

To complicate matters, spin-1/2 electrons and holes form $J=1$ orthoexcitons and $J=0$ paraexcitons, split by an exchange energy of 12 meV, with the paraexciton lying lowest. The rate equations for orthoexciton and paraexciton densities are

$$\frac{dn_o}{dt} = -\frac{n_o}{\tau} - A_{oo}n_o^2 - Dn_o + Un_p, \quad (2)$$

$$\frac{dn_p}{dt} = -\frac{n_p}{\tau} - A_{pp}n_p^2 + Dn_o - Un_p. \quad (3)$$

The A_{oo} and A_{pp} terms represent two types of Auger events that can occur between orthoexcitons and paraexcitons. $A_{op}n_on_p$ is also possible, as discussed in Ref. 10. D and U are the down-conversion and up-conversion rates between orthoexcitons and paraexcitons. Fortunately, the interconversion process has been isolated by experiments at low gas densities.¹¹ Also, in the “high temperature” experiments of Fig. 1, the exciton gas is in good thermal equilibrium with the lattice (as shown by the spectrum), and the orthoexcitons and paraexcitons have reached internal equilibrium ($n_o = 3n_p e^{-\Delta/k_B T}$), greatly simplifying the analysis.¹⁰

A representative $A(T)$ from the data analysis is plotted in Fig. 1(b), along with theoretical curves based on a calculation by Kavoulakis and Baym.¹² The Auger constant is found to vary roughly as $1/T$ between 70 K and 210 K, in contrast to the theoretical predictions for direct and phonon-assisted processes. Most surprising, experiment and theory differ by over five orders of magnitude.

These huge discrepancies suggest that the excitons are more strongly correlated than expected for a homogeneous ideal gas. Up to this point, the exciton gas in Cu₂O has been assumed to be a noninteracting gas in the thermodynamic sense; that is, there is little tendency for the excitons to bind into molecules or form electron-hole liquid. The basis for this assumption stems from both experiment and theory: (a) there is little spectral evidence for biexcitons (or liquid) in this crystal,¹³ and (b) prior theoretical estimates have predicted little or no molecular binding in Cu₂O.

The weakness of the molecular bond in Cu₂O stems in part from the relatively large mass ratio of electrons and holes ($\sigma = m_h/m_e = 0.59$), combined with a large exchange splitting Δ . Using a variational method, Bassani and Rovere¹⁴ predicted a biexciton binding energy $\phi < 0.2$ meV. Using a path integral approach, Huang¹⁵ calculates a binding energy of 13 meV, which is still a small value compared to the exciton binding energy $E_x = 153$ meV. A comparison of

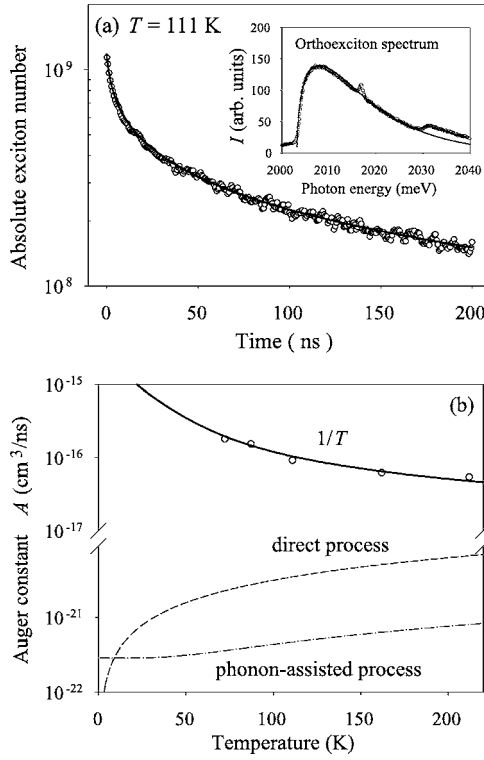


FIG. 1. (a) Total exciton transient ($n_o + n_p$) at 111 K showing a fast density-dependent decay rate following the 5 ps laser pulse. The best fit to the data (solid curve) follows from Eqs. (4). The inset shows the corresponding orthoexciton spectrum. (b) The measured Auger constant A as a function of T (circles). The solid curve is $1/T$. Theoretical Auger constants for direct (dashed) and phonon-assisted (dash-dotted) processes are based on the theory of Refs. 10 and 12.

the two theoretical approaches for various materials¹⁶ favors the latter approach. The biexciton has possible symmetries $\Gamma_1 + \Gamma_3 + \Gamma_4 + \Gamma_5$ corresponding to para-para and three ortho states.¹⁴ The Γ_1 ground state is radiatively forbidden.

We propose that the rapid decay of excitons is due to their capture into biexcitons, whose intrinsic lifetime is limited by a fast Auger recombination. The intermolecular Auger process should exhibit a huge enhancement due to the large effective density of the molecule, roughly $n_{\text{eff}} = (\phi/E_x) a_B^{-3}$, which implies subnanosecond biexciton lifetimes.¹⁷

In addition to particle loss, the Auger process (whether exciton or biexciton driven) causes heating of the exciton gas and regeneration of both ortho- and paraexcitons. These effects are best observed at crystal temperatures T_L below about 20 K, where (unfortunately) the orthoexciton and paraexciton populations are not described by thermal equilibrium. We denote T as the gas temperature. For low temperatures ($T_L < 20$ K), the rate equations for ortho-, para-, and biexcitons are most simply written as

$$\frac{dn_b}{dt} = -\frac{n_b}{\tau_A} + C'n_o^2 + Cn_p^2 - Cn^*n_b,$$

$$\frac{dn_o}{dt} = \frac{3n_b}{4\tau_A} - \frac{n_o}{\tau} - 2Bn_o^2 - Dn_o - 2C'n_o^2 + G,$$

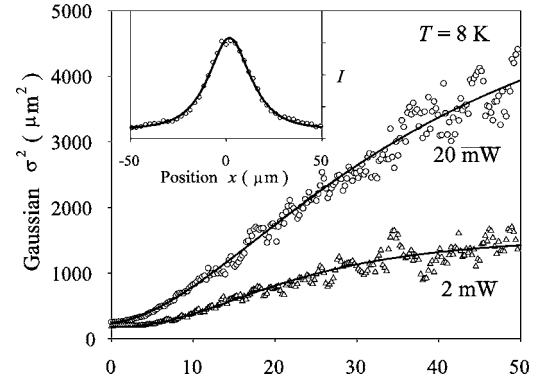


FIG. 2. Lateral expansion of exciton gas derived from spatial profiles of luminescence (inset). Complex diffusion and capture processes for orthoexcitons and paraexcitons are characterized by empirical fits (solid curves). With corresponding depth distributions (Ref. 10), the effective volume $V(t)$ is determined.

$$\frac{dn_p}{dt} = \frac{1}{4} \frac{n_b}{\tau_A} - \frac{n_p}{\tau} + 2Bn_o^2 + Dn_o - 2Cn_p^2 + 2Cn^*n_b. \quad (4)$$

In these equations, $C(C')$ is the para-para (ortho-ortho) capture coefficient, D is the phonon-assisted down-conversion rate, τ is the impurity-induced recombination time, and G is the optical generation rate. The scattering of two orthoexcitons with mutual spin-flip leaves two paraexcitons at a rate Bn_o . This density-dependent spin-flip process¹⁸ is also active at higher temperatures but it simply assists the thermal equilibrium between ortho and paraexcitons. The intrinsic Auger lifetime of biexcitons is designated as τ_A . The fractions $3/4$ and $1/4$ are due to $J=1$ and $J=0$ degeneracies. The mass-action equilibrium constant is given by

$$n^* = \frac{(n_o + n_p)^2}{n_b} = \left(\frac{mk_B T}{4\pi\hbar^2} \right)^{3/2} e^{-\phi/k_B T}, \quad (5)$$

where the biexciton mass is assumed to be twice as large as the exciton mass m . In our analysis, we use $B = 1.67 \times 10^{-16} \text{ cm}^3/\text{ns}$, based on a calculation by Kavoulakis and Mysyrowicz.^{18,19} The remaining parameters that must be determined from experiment are the biexciton binding energy ϕ , the biexciton Auger rate τ_A^{-1} , and the exciton capture coefficient C . The biexciton decay rate is not directly dependent on gas density, but the Auger matrix element is proportional to the center-of-mass momentum of the combining excitons, implying a temperature dependence $\tau_A^{-1} = aT$, with the coefficient a determined from our low-temperature data as described below.

We have measured time-resolved spectra for orthoexcitons at lattice temperatures of $T_L = 2, 8,$ and 14 K to determine the gas temperature during the decay process. Unlike the 70–210 K cases of Fig. 1(a), the exciton gas temperatures differ significantly from the lattice temperature at early times. Spectrally integrated spatial scans were also recorded. We used a 5 ps dye laser (repetition rate 9.6 MHz) adjusted throughout for an absorption length of $80 \mu\text{m}$. Figure 2 shows a typical gas expansion and Fig. 3 shows the exciton numbers $N_o(t)$ and $N_p(t)$ for the two species at $T_L = 8$ K at

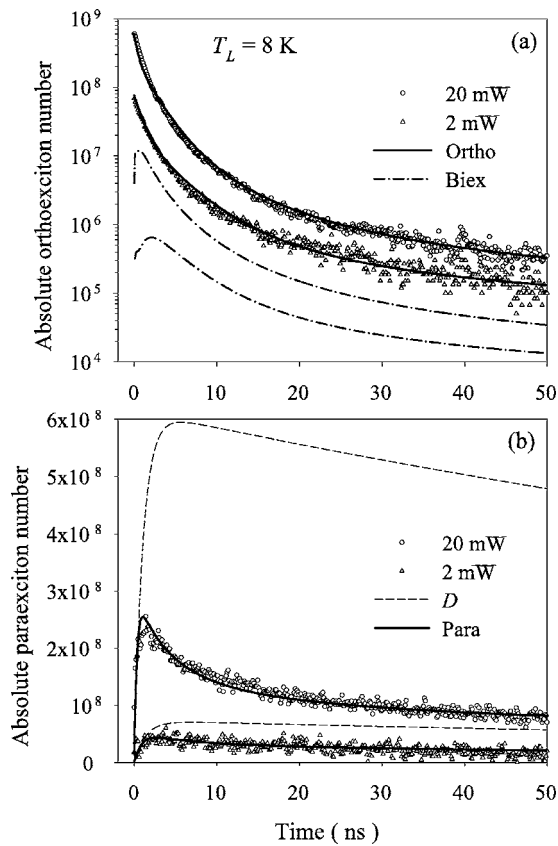


FIG. 3. (a) Observed decay of orthoexciton numbers at $T_L=8$ K for 2 and 20 mW excitation powers (time averaged). (b) Corresponding paraexciton transients scaled by a factor of 500, the ratio of ortho-para radiative rates. The solid curves are fits to orthoexciton and paraexciton transients, obtained by numerically solving the simultaneous rate Eqs. (4). The dash-dotted curves in (a) are predicted biexciton transients at each excitation level. The dashed curves in (b) correspond to the paraexciton buildups if there were no Auger decay or spin-flip scattering. Inclusion of the latter process causes a slight increase in the paraexciton buildup rate (dashed curve).

each excitation level. The two solid curves in Figs. 3(a) and 3(b) represent a single best fit to Eqs. (4). A clear indicator of the Auger process is the long tail of orthoexciton numbers in Fig. 3(a). At 8 K the up conversion from paraexcitons is negligible, so this late-time “regeneration” of orthoexcitons is a direct measure of the intrinsic Auger decay rate of biexcitons, $\tau_A^{-1}=0.5T \text{ ns}^{-1} \text{ K}^{-1}$.²⁰

The fast initial decay of orthoexcitons results mainly from capture into biexcitons ($Cn_o/3$). We have assumed that the orthoexciton capture constant (C') is three times smaller than for paraexcitons (C), due to spin degeneracy.¹⁹ Both orthotransients and paratransients are explained very well with these parameters over $T_L=2\text{--}14$ K range. The two-body spin-flip conversion to paraexcitons (Bn_o) with B given above has little effect.²¹ As seen in Fig. 3(b), the paraexciton numbers build up and then decay due to capture into biexcitons. The dashed lines show the predicted rate if there were no density-dependent processes, showing paraexciton production by ortho down-conversion and paraexciton decay at impurities.

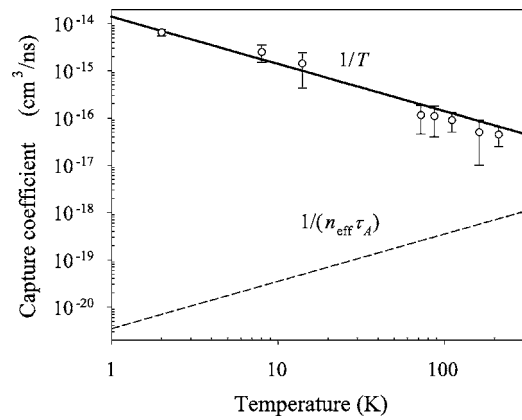


FIG. 4. Measured temperature dependence of the capture coefficient C , Eq. (6), evaluated at gas temperature $T=T_L$. In the fitting process, we assume an Auger constant for biexcitons $1/(n_{\text{eff}}\tau_A)$ as defined in the text.

The dash-dotted curves in Fig. 3(a) give the predicted biexciton numbers, showing in part why biexciton luminescence is not observed. The predicted biexciton numbers are much lower than the exciton numbers, and the radiative recombination of a biexciton in its ground state is highly forbidden. Due to rapid exciton capture and biexciton recombination, the exciton transients at low temperatures do not depend significantly on the biexciton binding energy ϕ .

However, given the biexciton Auger rate from the low-temperature data, we extract a biexciton binding energy $\phi=10$ meV from the exciton transients at high temperatures (e.g., Fig. 1). Varying the Auger rate up and down by a factor of two causes ϕ to vary over the range 8–15 meV with acceptable agreement between theory and experiment.

With the biexciton binding energy of 10 meV and the Auger rate given above, the capture coefficient over the 2–210 K range is

$$C(T) \approx \frac{(1.4 \pm 0.5) \times 10^{-14}}{T(\text{K})} \text{ cm}^3/\text{ns}, \quad (6)$$

which is consistent with our entire range of excitation levels, 2–20 mW. The temperature in this equation is the exciton gas temperature, which differs from the lattice temperature for data below $T_L=20$ K. Under these conditions, the gas temperatures T are determined from time-resolved spectra, and these temperatures are used to determine the instantaneous values of C in the numerical analysis. In Fig. 4 we plot Eq. (6) evaluated at $T=T_L$. Also shown is the effective Auger constant for biexcitons from $An_{\text{eff}}=\tau_A^{-1}$.

One of the interesting findings is that the biexciton loss mechanism closely mimics the Auger decay of a noninteracting exciton gas. Specifically, for biexciton Auger decay rate (τ_A^{-1}) larger than the dissociation rate (Cn^*), the exciton capture coefficient (C) replaces the exciton Auger constant (A) in Eq. (1). A biexciton binding energy of only 10 meV is capable of reproducing the observed exciton dynamics over the experimental range.

We are led to the conclusion that capture of excitons into short-lived biexcitons is the principal loss mechanism of ex-

citons. Our analysis of optically inactive biexciton numbers [Fig. 3(a)] is consistent with the fact that biexcitons have never been directly observed in Cu_2O by photoluminescence. It may be possible, however, to create biexcitons by two-photon absorption and detect the orthoexciton and paraexciton Auger byproducts.

This material is based upon work supported by the U.S. Department of Energy, Division of Materials Sciences under Contract No. DEFG02-91ER45439, through the Frederick Seitz Materials Research Laboratory at the University of Illinois at Urbana-Champaign. Experiments were conducted in the MRL Laser and Spectroscopy Facility.

-
- ¹D. Hulin, A. Mysyrowicz, and C. Benoît à la Guillaume, *Phys. Rev. Lett.* **45**, 1970 (1980); J. P. Wolfe, J. L. Lin, and D. W. Snoke in *Bose-Einstein Condensation*, edited by A. Griffin, D. W. Snoke, and S. Stringari (Cambridge University Press, Cambridge, 1995).
- ²N. Naka, S. Kono, M. Hasuo, and N. Nagasawa, *Prog. Cryst. Growth Charact.* **33**, 89 (1996).
- ³M. Y. Shen, T. Yokouchi, S. Koyama, and T. Goto, *Phys. Rev. B* **56**, 13 066 (1997).
- ⁴K. E. O'Hara, L. Ó. Súilleabháin, and J. P. Wolfe, *Phys. Rev. B* **60**, 10 565 (1999).
- ⁵K. E. O'Hara, J. R. Gullingsrud, and J. P. Wolfe, *Phys. Rev. B* **60**, 10 872 (1999).
- ⁶K. E. O'Hara and J. P. Wolfe, *Phys. Rev. B* **62**, 12909 (2000).
- ⁷D. W. Snoke and V. Negoita, *Phys. Rev. B* **61**, 2904 (2000).
- ⁸S. Denev and D. W. Snoke, *Phys. Rev. B* **65**, 085211 (2002).
- ⁹A. Jolk, M. Jörger, and C. Klingshirn, *Phys. Rev. B* **65**, 245209 (2002).
- ¹⁰J. P. Wolfe and J. I. Jang, *Solid State Commun.* **134**, 143 (2005).
- ¹¹J. I. Jang, K. E. O'Hara, and J. P. Wolfe, *Phys. Rev. B* **70**, 195205 (2004).
- ¹²G. M. Kavoulakis and G. Baym, *Phys. Rev. B* **54**, 16 625 (1996). The deformation potential $D_{12} \approx 2.5 \text{ eV}/\text{Å}$ used by these authors to predict $A \approx 5 \times 10^{-19} \text{ cm}^3/\text{ns}$ at zero T was based on an incorrect value of the paraexciton radiative lifetime. An experimental value of $D_{12} \approx 0.12 \text{ eV}/\text{Å}$ by D. W. Snoke, D. Braun, and M. Cardona, *Phys. Rev. B* **44**, 2991 (1991) yields a far smaller Auger constant, $A \approx 10^{-21} \text{ cm}^3/\text{ns}$.
- ¹³Y. Petroff, P. Y. Yu, and Y. R. Shen, *Phys. Rev. Lett.* **29**, 1558 (1972).
- ¹⁴F. Bassani and M. Rovere, *Solid State Commun.* **19**, 887 (1976). The authors used an exchange energy $|J| = 100\text{--}600 \text{ meV}$, much larger than an updated value of 23 meV (Ref. 11).
- ¹⁵W.-T. Huang, *Phys. Status Solidi B* **60**, 309 (1973). The value of 13 meV corresponds to $\sigma = 0.58$ in Fig. 1.
- ¹⁶C. Klingshirn and H. Haug, *Phys. Rep.* **70**, 315 (1981).
- ¹⁷This formula naively assumes a van der Waals bonding of excitons. The actual electronic structure of a biexciton is unknown.
- ¹⁸G. M. Kavoulakis and A. Mysyrowicz, *Phys. Rev. B* **61**, 16 619 (2000).
- ¹⁹The process only occurs for two oppositely spin-aligned orthoexcitons, causing a statistical factor of 1/3.
- ²⁰This rate is 70 times larger than An_{eff} obtained from the theoretical estimate $A = 8 \times 10^{-21} \text{ cm}^3/\text{ns}$ at 210 K [see Fig. 1(b)] and the simple van der Waals estimate $n_{\text{eff}} = (\phi/E_x)a_B^{-3}$ with $\phi = 10 \text{ meV}$. However, the estimate of A is highly uncertain due to large exponents in the theoretical expression (Ref. 12). For example, this discrepancy could be resolved by assuming a dipole moment between opposite-parity bands 2.9 times larger than quoted in Ref. 12.
- ²¹M. Kubouchi, K. Yoshioka, R. Shimano, A. Mysyrowicz, and M. Kuwata-Gonokami, *Phys. Rev. Lett.* **94**, 016403 (2005). Using infrared spectroscopy, these researchers measured orthotransients and paratransients following two-photon excitation. From the paraexciton buildup, they extract a value of B that is 18 times larger than the value we use; however, their orthoexciton decay rate [Fig. 4(a)] seems consistent with D in our Eqs. (4).